Available online at www.sciencedirect.com
SCIENCE DIRECT®
Journal of Non-Crystalline Solids 345&346 (2004) 518–522
JOURNAL OF NON-CRYSTALLINE SOLIDS
www.elsevier.com/locate/jnoncrysol

# Convolution and renormalization techniques applied to the Kubo conductivity in quasiperiodic systems

Vicenta Sánchez ☆, Chumin Wang *

*Instituto de Investigaciones en Materiales, Universidad Nacional Autó noma de México, Apartado Postal 70-360, México D.F. 04510, Mexico*

Available online 6 October 2004

**Abstract**

The localization and transport properties in quasiperiodic systems are quite different from those in crystalline and in disordered materials. In this work, we study the electrical conduction in macroscopic Fibonacci lattices by using the Kubo–Greenwood formula and a single-band tight-binding model. This study is carried out by means of the convolution technique and a novel renormalization method, which allows iterative evaluation of the products of the Green's function in an exact way. The results of the spectrally averaged conductance show a power-law decay as the length of the quasiperiodic systems increases along the applied electric field. This fact reveals the critical localization nature in quasicrystalline materials, contrary to the constant and exponencial decay behaviors found in the periodic and randomly disordered systems, respectively.


*PACS:* 71.23.Ft; 72.15.−v

## 1. Introduction

Quasicrystals are materials that have a long-range rotational symmetry and an aperiodic atomic order [1]. They possess unusual transport properties, e.g., extremely low conductivity for alloys of metallic constituents [2], which are believed to be consequence of the quasiperiodicity of the system. Nowadays, there is a consensus that in the quasiperiodic systems the electronic wave functions are critical, neither localized nor extended, and the corresponding eigenvalue spectra are singular continuous [3]. Hence, the transport properties of these critically localized states are a fascinating and still unclear subject. Moreover, the level-spacing statistics show an inverse-power-law distribution of gaps [4,5] and a semi-Poisson distribution of bands [6], both neither conventional Poisson nor Wigner ones. In the last decade, numerical studies of electron transport properties have been carried out in approximants [7], due to the absence of reciprocal lattice for quasiperiodic systems. Recently, we have developed a new renormalization method for the Kubo–Greenwood formula in Fibonacci chains [8], in order to analyze transport behaviors in macroscopic systems. This method can be extended to the bond problem [9].

In general, the Fibonacci sequence ($F_n$) of generation $n$ can be built by defining $F_1 = A$, $F_2 = BA$, and the addition rule, $F_n = F_{n-1} \oplus F_{n-2}$, understood as the joining of sequences. For instance, $F_4 = BAABA$. For the bond problem, studied in this paper, the on-site energies are the same and the hopping integrals, $t_A$ (thick lines in Fig. 1) and $t_B$ (thin lines in Fig. 1), are organized following the Fibonacci sequence. On the other hand, a two-dimensional (2D) Fibonacci superlattice can be built by stacking periodically Fibonacci chains, connected

☆ Present address: Departamento de Física, Facultad de Ciencias, Universidad Nacional Autónoma de México, Apartado Postal 70-542, México D.F. 04510, México.
* Corresponding author. Tel.: +52 55 56224634; fax: +52 55 56161251.
*E-mail address:* chumin@servidor.unam.mx (C. Wang).

0022-3093/$ - see front matter © 2004 Elsevier B.V. All rights reserved.
doi:10.1016/j.jnoncrysol.2004.08.077

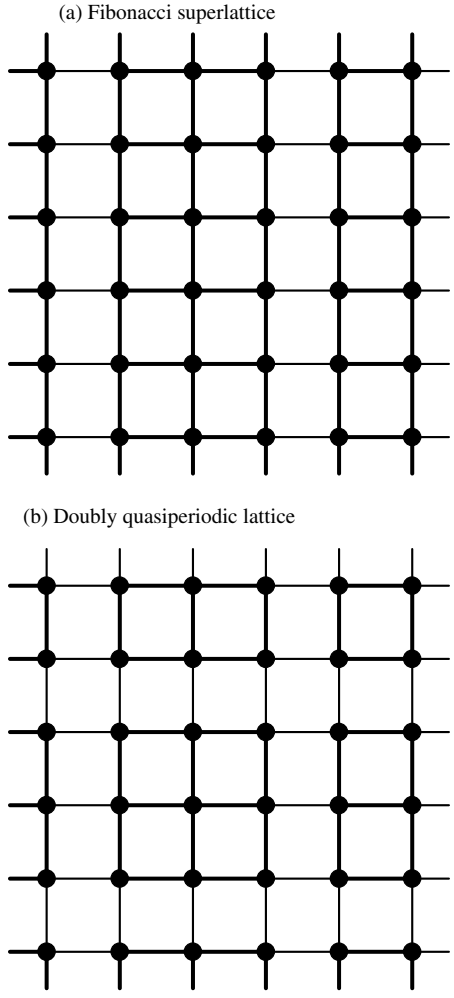


Fig. 1. (a) Two-dimensional Fibonacci superlattice and (b) doubly quasiperiodic lattice, both with null on-site energies and two kinds of hopping integrals $t_A$ (thick lines) and $t_B$ (thin lines).

by the same hopping integrals $t = t_A$, as shown in Fig. 1(a). The doubly quasiperiodic lattices are constructed following the Fibonacci sequence in both directions (see Fig. 1(b)).

In the linear response theory, the real part of the electrical conductivity ($\sigma$) is given by the Kubo–Greenwood formula [10]

$$\sigma(\mu,\omega,T) = \lim_{\substack{\Omega\to\infty \\ \eta\to 0^+}} \frac{2e^2\hbar}{\pi\Omega m^2} \int_{-\infty}^{\infty} dE \frac{f(E) - f(E+\hbar\omega)}{\hbar\omega} \times Tr[p\mathrm{Im}G^+(E+\hbar\omega+i\eta)p\mathrm{Im}G^+(E+i\eta)], \quad (1)$$

where $\Omega$ is the volume of the system, $G^+(E)$ is the retarded one-particle Green's function, $p = \frac{ima}{\hbar}\sum_j\{t_{j,j+1} \mid j\rangle\langle j+1 \mid - t_{j,j-1} \mid j\rangle\langle j-1 \mid\}$ is the projection of the momentum operator along the applied electric field with frequency $\omega$, and $f(E) = \{1 + \exp[(E-\mu)/k_BT]\}$ is the Fermi–Dirac distribution with Fermi energy $\mu$ and temperature $T$.

In this paper, we report an analysis of the two- and three-dimensional (3D) electrical conductance, $g(\mu) = \sigma(\mu)W_\perp/L_\parallel$, where $W_\perp = N_\perp a^2$ and $L_\parallel = N_\parallel a$ are respectively the cross-section area and the length of the system in reference of the applied electric field, i.e., $\Omega = W_\perp L_\parallel$. In the Appendix A, we show that when the Hamiltonian of the system ($H$) is separable, i.e., $H = H_\parallel \otimes I_\perp + I_\parallel \otimes H_\perp$, being $I$ the identity matrix, the conductivity ($\sigma$) can be calculated by using the convolution technique

$$\sigma(\mu,\omega,T) = \frac{1}{W_\perp}\sum_\beta \sigma^\parallel(\mu - E_\beta,\omega,T), \quad (2)$$

where $\sigma^\parallel$ is the single-chain one-dimensional (1D) conductivity along the electric field and $E_\beta$ are the eigenvalues of the 2D cross-section Hamiltonian ($H_\perp$).

In the following section, the electric conductance of different systems and its spectral averages as a function of the length of the quasiperiodic systems are investigated.

## 2. Results

The dc conductances [$g(\mu)$] at zero temperature as a function of the Fermi energy ($\mu$) are shown in Fig. 2(a) for a 2D periodic lattice with $W_\perp = 22$ atoms, hopping integrals $t$, null on-site energies and arbitrary value of $L_\parallel$, 2(b) for a 2D Fibonacci superlattice, which is periodic along the applied electric field and quasiperiodic in the other direction, and 2(c) for the same Fibonacci superlattice, except the quasiperiodic order is now along the applied electrical field. In Fig. 2(b) and (c), the 2D lattice is built by 514 230 (periodically ordered) × 46 369 (quasiperiodically ordered) atoms with null on-site energies, hopping integrals $t_A = t$ and $t_B = \tau t$ for the quasiperiodic direction, being $\tau = (\sqrt{5}-1)/2$. Along the applied electric field the systems are connected to two semi-infinite periodic leads with hopping integrals $t$, in order to simulate experimental conditions. The imaginary part of the energy ($\eta$) in these figures is $10^{-11}|t|$. Fig. 2(b′), inset of Fig. 2(b), shows an enlarged portion of the $g(\mu)$ curve.

In order to analyze global properties of the spectra, an spectral average of the conductance ($\langle g\rangle$) is defined as

$$\langle g\rangle = \frac{\int dE\, g(E)\mathrm{DOS}(E)}{\int dE\, \mathrm{DOS}(E)}. \quad (3)$$

where DOS($E$) is the density of states of the system. $\langle g\rangle$ versus the system length ($L_\parallel$) are shown in Fig. 3(a) for Fibonacci superlattices with 1D cross sections of $W_\perp = 35$ atoms (open triangles) and of $W_\perp = 1225$ atoms (open circles), and with a 2D cross section of $W_\perp = 1225$ atoms (open squares). Fig. 3(b) shows the same graph as in Fig. 3(a), except for systems where the quasiperiodic order is in every direction. In Fig. 3

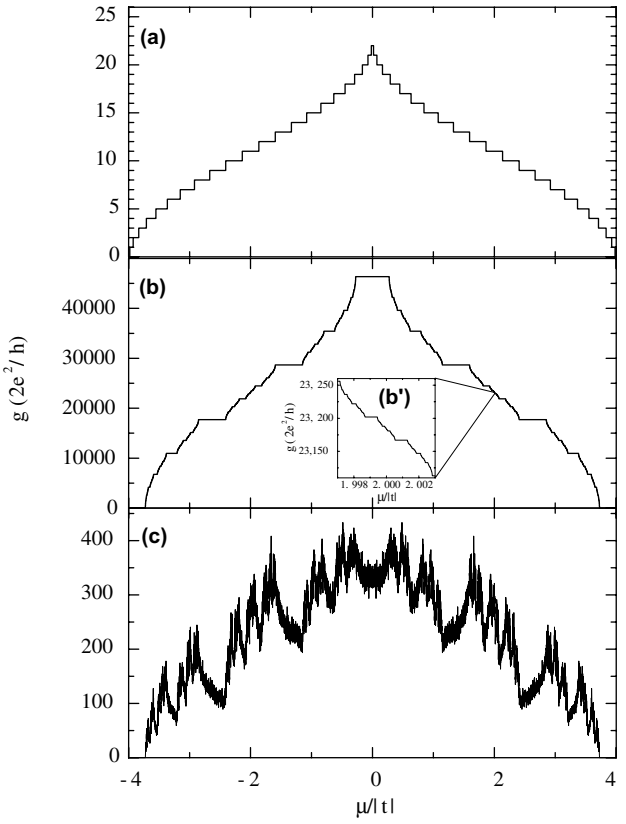


Fig. 2. The dc conductances [$g(\mu)$] at zero temperature as a function of the Fermi energy ($\mu$) for (a) a 2D periodic lattice, (b) and (c) the same 2D Fibonacci superlattice, where the quasiperiodic order is perpendicular and along the applied electrical field, respectively. In Fig. 2(b) and (c) the Fibonacci chains have null on-site energies, hopping integrals $t_A = t$ and $t_B = \tau t$. Along the applied electric field the systems are connected to two periodic semi-infinite leads. An amplification of the conductance spectrum is shown in Fig. 2(b′).

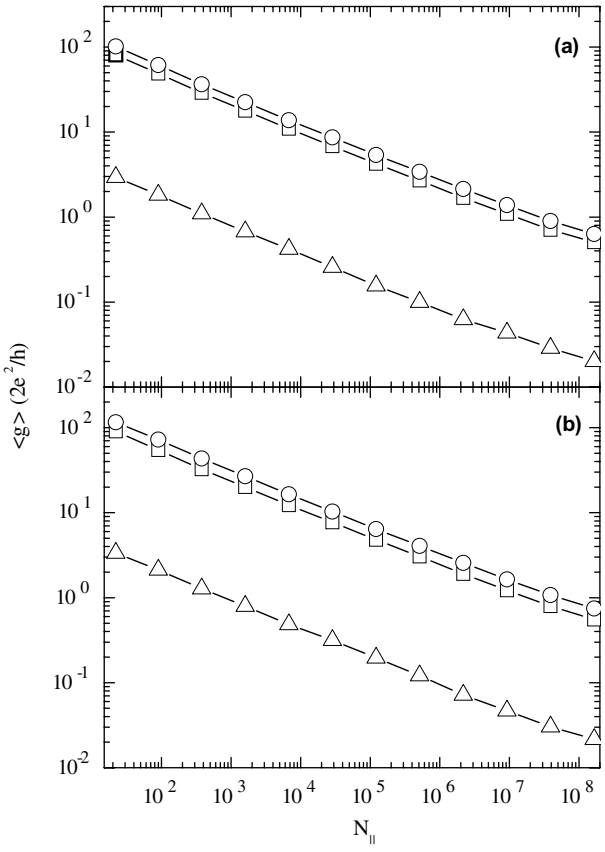


Fig. 3. Spectrally averaged conductance ($\langle g\rangle$) as a function of the number of atoms along the applied electric field ($N_{\|}$) for Fibonacci superlattices with 1D cross sections of $W_{\perp} = 35$ atoms (△) and of $W_{\perp} = 1225$ atoms (○), and with a 2D cross section of $W_{\perp} = 1225$ atoms (□). Fig. 3(b) shows the same graph as in Fig. 3(a), except that the quasiperiodic order is in every direction. In Fig. 3 the Fibonacci sequences are built by using the same parameters of Fig. 2.

the Fibonacci sequences are built by using the same parameters of Fig. 2.

## 3. Discussion

Observe that for 2D periodic lattices the dc conductance has well defined quantum steps in units of $2e^2/h$ (see Fig. 2(a)), as observed firstly in point contacts [11] and recently in ballistic quantum wires [12]. When the quasiperiodicity is introduced in the perpendicular direction to the applied electric field, a self-similar stair structure is observed (see Fig. 2(b) and (b′)), despite that the height of the steps remains the same unit of $2e^2/h$. Now, if the electric field is applied to the same system as in Fig. 2(b), but along the direction of quasiperiodic order, the conductance spectra become totally different, showing a spiky structure.

To analyze these 'noisy' spectra an average of conductance is introduced in Eq. (3) Notice in Fig. 3 that $\langle g\rangle$ decays following a power law [$\langle g\rangle = 2e^2(\alpha N_{\|}^{-\nu})/h$] when the system length increases, as reported for finite Penrose lattices [13], contrary to the constant behaviors in periodic systems. We found $\nu = 0.32341$ and $\alpha = 198.76962$ for 3D Fibonacci superlattices (open squares), $\nu = 0.3231$ and $\alpha = 250.12667$ for 2D Fibonacci superlattices (open circles), $\nu = 0.31889$ and $\alpha = 7.2041$ for 2D Fibonacci superlattices (open triangles), $\nu = 0.32375$ and $\alpha = 224.00618$ for 3D triply quasiperiodic lattices (open squares), $\nu = 0.32189$ and $\alpha = 292.94089$ for 2D doubly quasiperiodic lattices (open circles), $\nu = 0.32374$ and $\alpha = 8.75709$ for 2D doubly quasiperiodic lattices (open triangles). Summarizing these numerical data, it can be observed that for the same number of atoms in the cross section less connection between chains leads to a larger spectrally-averaged conductance. For instance, $\langle g\rangle$ of a 2D system (open circles) is larger than those of a 3D one (open squares), having the same cross-section area. Moreover, the averaged conductance of Fibonacci superlattices are smaller than those of doubly or triply quasiperiodic lattices, possibly originated from the better structural coherence in the multiply quasiperiodic systems.

## 4. Conclusions

We have studied the electronic transport in macroscopic Fibonacci systems within the Kubo–Greenwood formulation. This study is done by using a novel renormalization method and convolution technique for calculations of the electrical conductivity in two- and three-dimensional systems. It would be important to stress that these calculations have been carried out without approximations within the Kubo–Greenwood formalism. However, the convolution technique is applicable only when the Hamiltonian of the system is separable. On the other hand, the length dependence shows power-law decays of the spectrally averaged conductance, revealing the critical localization nature of the wave functions in quasiperiodic systems, contrary to the constant and exponential decay behaviors in the periodic and randomly disordered systems, respectively [15].

## Acknowledgments

This work has been supported partially by CONACyT-41492-F, DGAPA-IN122704, and DGAPA-IN101701. Computations have been performed at the Bakliz of DGSCA, UNAM.

## Appendix A. Convolution Method

For a given Hamiltonian $H$, the corresponding Green's function ($G$) can be expressed as

$$G_{lk}(z) = \sum_{\alpha} \frac{\langle l \mid \alpha\rangle\langle \alpha \mid k\rangle}{z - E_\alpha}, \tag{A.1}$$

where the eigenstates ($|\alpha>$) are determined by $H|\alpha> = E_\alpha|\alpha>$ and $z = E + i\eta$ is complex number. Eq. (A.1) cab be rewritten as

$$-\frac{1}{\pi}\mathrm{Im}[G_{lk}(z)] = \sum_{\alpha}\langle l \mid \alpha\rangle\langle \alpha \mid k\rangle\delta(E - E_\alpha), \tag{A.2}$$

since

$$\lim_{\eta\to 0}\frac{1}{x \pm i\eta} = P\left(\frac{1}{x}\right) \mp i\pi\delta(x). \tag{A.3}$$

If $H$ is separable, i.e., $H = H_{\|}\otimes I_\perp + I_{\|}\otimes H_\perp$, its eigenvalues and eigenfunctions can be respectively written as $E = E_\alpha + E_\beta$ and $|\alpha, \beta> = |\alpha>|\beta>$, where $H_{\|}|\alpha> = E_\alpha|\alpha>$ and $H_\perp|\beta> = E_\beta|\beta>$. Thus, the Green's function is given by

$$G_{(r,j)(k,l)}(z) = \sum_{\alpha,\beta}\frac{< r \mid \alpha >< \alpha \mid k >< j \mid \beta >< \beta \mid l >}{z - (E_\alpha + E_\beta)}, \tag{A.4}$$

where $r$ and $k$ are site coordinates in the parallel subspace, while $j$ and $l$ are site coordinates in the perpendicular subspace. Moreover, using Eq. (A.2) we have

$$\begin{aligned}
&G_{(r,j)(k,l)}(z+\hbar\omega)\\
&\quad= \int_{-\infty}^{\infty}\mathrm{d}y\sum_{\alpha,\beta}\frac{< r|\alpha >< \alpha|k >< j|\beta >< \beta|l >}{z+\hbar\omega-(E_\alpha+y)}\\
&\qquad\times\delta(y-E_\beta)\\
&\quad= -\frac{1}{\pi}\lim_{\eta'\to 0}\int_{-\infty}^{\infty}\mathrm{d}y\sum_{\alpha}\frac{< r \mid \alpha >< \alpha|k >}{z+\hbar\omega-(E_\alpha+y)}\\
&\qquad\times\mathrm{Im}\left[G^{\perp}_{jl}(y+i\eta')\right]\\
&\quad= -\frac{1}{\pi}\lim_{\eta'\to 0}\int_{-\infty}^{\infty}\mathrm{d}y G^{\|}_{rk}(z+\hbar\omega-y)\mathrm{Im}\left[G^{\perp}_{jl}(y+i\eta')\right].
\end{aligned} \tag{A.5}$$

In the Kubo–Greenwood formula (Eq. (1)), the projection of the momentum operator ($p$) is along the applied electric field, i.e., $p_{(k,l)(f,s)} = p^{\|}_{kf}\delta_{l,s}$ is in the parallel subspace. Using equations (A.5) and (A.2) one obtains

$$\begin{aligned}
&Tr[p\mathrm{Im}G^{+}(z+\hbar\omega)p\mathrm{Im}G^{+}(z)]\\
&\quad= \sum_{r,j,k,l,f,s,v,w}\left\{p_{(v,w)(r,j)}\mathrm{Im}\left[G_{(r,j)(k,l)}(z+\hbar\omega)\right]p_{(k,l)(f,s)}\right.\\
&\qquad\left.\times\mathrm{Im}\left[G_{(f,s)(v,w)}(z)\right]\right\}\\
&\quad= \sum_{r,j,k,l,f,v}\left\{p^{\|}_{vr}\mathrm{Im}\left[G_{(r,j)(k,l)}(z+\hbar\omega)\right]p^{\|}_{kf}\mathrm{Im}\left[G_{(f,l)(v,j)}(z)\right]\right\}\\
&\quad= \frac{1}{\pi^2}\sum_{r,j,k,l,f,v}p^{\|}_{vr}\int_{-\infty}^{\infty}\mathrm{d}x\,\mathrm{Im}\left[G^{\|}_{rk}(z+\hbar\omega-x)\right]\\
&\qquad\times\mathrm{Im}\left[G^{\perp}_{jl}(x+i\eta')\right]p^{\|}_{kf}\int_{-\infty}^{\infty}\mathrm{d}y\,\mathrm{Im}\left[G^{\|}_{fv}(z-y)\right]\\
&\qquad\times\mathrm{Im}\left[G^{\perp}_{lj}(y+i\eta'')\right]\\
&\quad= \sum_{r,j,k,l,f,v}\int_{-\infty}^{\infty}\mathrm{d}x\int_{-\infty}^{\infty}\mathrm{d}y\,p^{\|}_{vr}\mathrm{Im}\left[G^{\|}_{rk}(z+\hbar\omega-x)\right]p^{\|}_{kf}\\
&\qquad\times\mathrm{Im}\left[G^{\|}_{fv}(z-y)\right]\\
&\qquad\times\left[\sum_{\beta'}< j \mid \beta' >< \beta' \mid l > \delta(x-E_{\beta'})\right]\\
&\qquad\times\left[\sum_{\beta}< l \mid \beta >< \beta \mid j > \delta(y-E_\beta)\right]\\
&\quad= \sum_{r,k,f,v}\int_{-\infty}^{\infty}\mathrm{d}y\,p^{\|}_{vr}\mathrm{Im}\left[G^{\|}_{rk}(z+\hbar\omega-y)\right]p^{\|}_{kf}\\
&\qquad\times\mathrm{Im}\left[G^{\|}_{fv}(z-y)\right]\left[\sum_{\beta}\delta(y-E_\beta)\right].
\end{aligned} \tag{A.6}$$

Therefore, considering $\mathrm{DOS}^{\perp}(y) = \sum_{\beta}\delta(y - E_{\beta})$, we obtain the well known convolution relationship [14]

$$\sigma(E,\omega,T) = \frac{1}{\Omega_{\perp}}\int_{-\infty}^{\infty} \mathrm{d}y\sigma^{\parallel}(E-y,\omega,T)\mathrm{DOS}^{\perp}(y), \quad \text{(A.7)}$$

where

$$\sigma^{\parallel}(E,\omega,T) = \lim_{\substack{\Omega\to\infty \\ \eta\to 0^{+}}} \frac{2e^2\hbar}{\pi\Omega_{\parallel}m^2}\int_{-\infty}^{\infty}\mathrm{d}E\frac{f(E)-f(E+\hbar\omega)}{\hbar\omega} \times \sum_{r,k,f,v} p^{\parallel}_{vr}\mathrm{Im}\left[G^{\parallel}_{rk}(z+\hbar\omega)\right]p^{\parallel}_{kf}\mathrm{Im}\left[G^{\parallel}_{fv}(z)\right]. \quad \text{(A.8)}$$

Finally, Eq. (9) can also be written as

$$\sigma(E,\omega,T) = \frac{1}{\Omega_{\perp}}\sum_{\beta}\sigma^{\parallel}(E-E_{\beta},\omega,T). \quad \text{(A.9)}$$

This last formulation could particularly be useful for systems with a small cross section perpendicular to the applied electric field, such as quantum wires and nanotubes.

## References

[1] C. Janot, Quasicrystal, Oxford University, New York, 1992.
[2] Z.M. Stadnik, Physical Properties of Quasicrystals, Springer, Berlin, 1999.
[3] A. Sütő, in: F. Axel, D. Gratias (Eds.), Beyond Quasicrystals, Les Editions de Physique, France, 1994, p. 483.
[4] K. Machida, M. Fujita, Phys. Rev. B 34 (1986) 7367.
[5] T. Geisel, R. Ketzmerick, G. Petschel, Phys. Rev. Lett. 66 (1991) 1651.
[6] S.N. Evangelou, J.-L. Pichard, Phys. Rev Lett. 84 (2000) 1643.
[7] U. Mizutani, T. Takeuchi, H. Sato, J. Phys.: Condens. Matter 14 (2002) R767.
[8] V. Sánchez, L.A. Pérez, R. Oviedo-Roa, C. Wang, Phys. Rev. B 64 (2001) 174205.
[9] V. Sánchez, C. Wang, J. Phys. Soc. Jpn. 72 (Suppl. A) (2003) 177.
[10] B. Kramer, A. MacKinon, Rep. Prog. Phys. 56 (1993) 1469.
[11] B.J. van Wees, H. van Houten, C.W.J. Beenakker, J.G. Williamson, L.P. Kouwenhoven, D. van der Marel, C.T. Foxon, Phys. Rev. Lett. 60 (1988) 848.
[12] R. de Picciotto, H.L. Stormer, L.N. Pfeiffer, K.W. Baldwin, K.W. West, Nature 411 (2001) 51.
[13] H. Tsunetsugu, K. Ueda, Phys. Rev. B 43 (1991) 8892.
[14] W.A. Schwalm, M.K. Schwalm, Phys. Rev. B 37 (1988) 9524.
[15] A. García-Martín, J.J. Sáenz, Phys. Rev. Lett. 87 (2001) 116603.